Amphiphilic Polymer Conetworks Studied by SANS: Effect of Type of Solubilisate and Molecular Architecture on the Swollen Gel Structure

Paula Malo de Molina[1,2,3]*, Demetris Kafouris[4], Costas S. Patrickios,[4] Laurence Noirez,[5] Michael Gradzielski[1]*

[1]: Stranski-Laboratorium für Physikalische und Theoretische Chemie; Institut für Chemie, Straße des 17. Juni 124, Technische Universität Berlin, D-10623 B
erlin, Germany

[2]: Centro de Física de Materiales (CFM), CSIC-UPV/EHU, San Sebastián, Spain

[3]: IKERBASQUE-Basque Foundation for Science, Bilbao, Spain

[4]: Department of Chemistry, University of Cyprus, P. O. Box 20537, 1678 Nicosia, Cyprus

[5]: Laboratoire Léon Brillouin (CEA-CNRS), Uni. Paris-Saclay, CEA-Saclay, 91191 Gif-sur-Yvette, France

Submitted for publication in

Macromolecules
14.06.2023

e-mail addresses:
P. Malo de Molina: p.malodemolina@ehu.eus
D. Kafouris: dkafouris@sgl.moh.gov.cy
C. S. Patrickios: costasp@ucy.ac.cy
L. Noirez: laurence.noirez@cea.fr
M. Gradzielski: michael.gradzielski@tu-berlin.de

*Authors to whom correspondence should be addressed.

Abstract

Amphiphilic polymer conetworks (APCNs) are hydrogels with hydrophobic regions synthesized by cross-linking well-defined copolymers. Due to their amphiphilicity, they have

oil solubilisation ability. In this paper, we present a small-angle neutron scattering (SANS) study of the oil solubilisation at the mesoscopic level in APCNs swollen in D_2O, where for better contrast conditions, the hydrophobic monomer (M) was deuterated. The study was carried out on a series of APCNs where we varied systematically the mole fraction of the hydrophobic methyl methacrylate (M) monomer repeating units (from 0.1 to 0.9) with respect to the hydrophilic 2-(dimethylamino)ethyl methacrylate (D) monomer repeating units, as well as the general block copolymer architecture (MDM *vs.* DMD). First, the structure of the D_2O-swollen APCNs was characterised by means of SANS, which showed a well-defined structure with a repeat spacing of the domains, d, that scales directly with the architecture of the building blocks of the APCNs. In the second step, the solubilisation of oils of different polarity (octane, toluene, eugenol, and 1-hexanol) was probed, and a clear correlation of oil solubilisation with the oil polarity was observed. The most unpolar oil, octane, did not solubilise at all, while the much more polar toluene and 1-hexanol were incorporated very well, but in a markedly different fashion. Toluene swelled completely the MMA part, while 1-hexanol appeared to be much more associated to the amphiphilic interface. This demonstrates that the studied APCNs are very selective with respect to their solubilisation properties and efficient for distinguishing different types of oils.

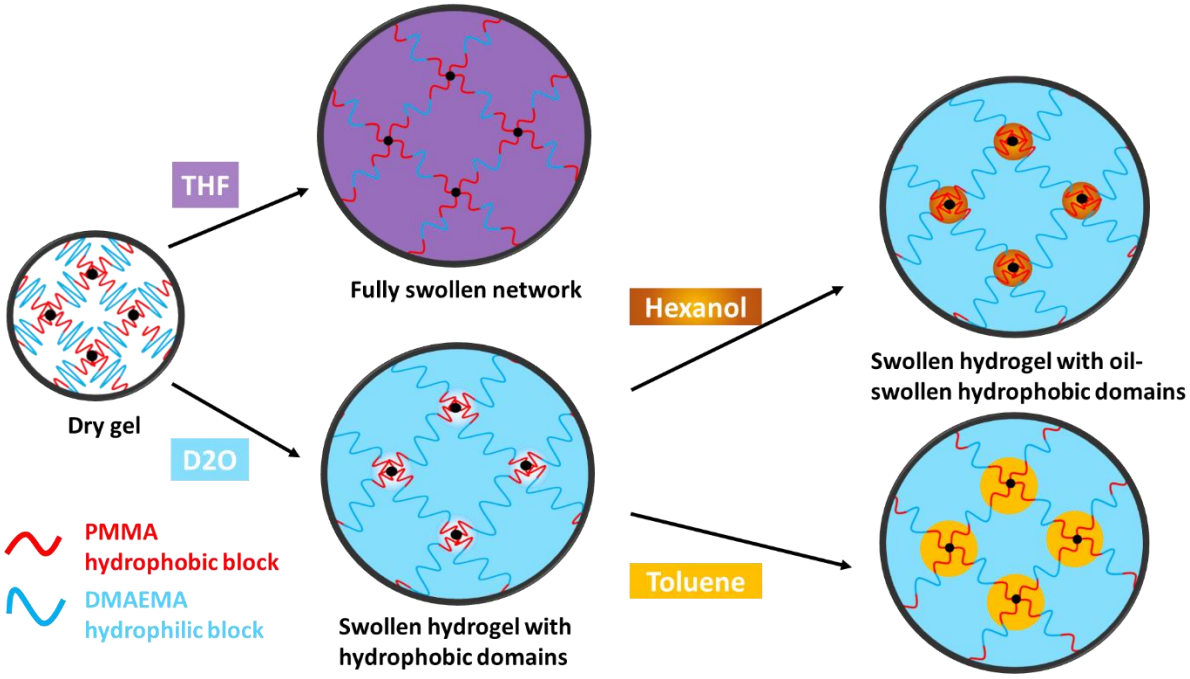

Keywords: Small-angle neutron scattering (SANS), amphiphilic polymer conetworks, APCNs, oil solubilisation, hydrogel.

Introduction

Solubilisation of oils in self-assembling amphiphilic systems is a well-established phenomenon for surfactants, where it leads to the formation of thermodynamically stable swollen micelles, microemulsions[1] or thermodynamically unstable emulsions.[2] More recently, the solubilisation in polymer surfactants or, in general, in amphiphilic block copolymers has been studied, and, in principle, similar mechanisms prevail here as in the case of low molecular weight amphiphiles. For instance, the formation of stable, microemulsion-type aggregates has been shown for poly(tert-butylstyrene)-b-poly(sodium styrene sulfonate) (PtBS-PSS) and cyclohexane in water.[3] For simple diblock and triblock copolymers, one may then have rather similar conditions as for normal surfactants; however, solubilisation in self-assembled polymeric systems may occur in more complex and constrained ways arising from the polymer architecture. The solubilisation properties of such copolymers have been studied already a long time ago theoretically[4] with the outcome of a high selectivity of solubilisation in block copolymer micelles[5] and such models can correlate solubilisation with detailed structural parameters of the micelles and the solvent quality of the different blocks for a given solubilisate.[6] Experimentally, some work has been dedicated to the solubilisation of conventional oils, as for instance in the case of poloxamer (PEO-PPO-PEO) micelles to extract aromatic hydrocarbons,[7] but most work has been dedicated to studying the solubilisation of drug molecules with the aim of using the copolymer micelles as drug delivery vehicles.[8]

A particular case for such an intricate situation is that of amphiphilic polymer conetworks (APCNs) made by cross-linking well-defined amphiphilic copolymers, where distinct hydrophilic and hydrophobic domains are present but their arrangement is substantially constrained by the polymeric network in which they are contained. APCNs have been the subject of a number of recent investigations[9–12] and have shown to be versatile soft-matter systems in which the properties of polymer networks, such as their elastic properties and rather high transparency, are combined with those of self-assembling systems. In recent years, we have prepared and investigated such APCNs based on MMA as hydrophobic and DMAEMA as hydrophilic moieties.[10,13]

Depending on the conetwork architecture, APCNs show microphase segregation in aqueous solution with more or less extended hydrophobic domains depending on the length of the hydrophobic blocks and the flexibility of the connecting hydrophilic chains.[14] Of course, such hydrophobic domains in copolymer networks will have the ability to solubilise hydrophobic

compounds in a similar fashion as surfactant micelles. Accordingly, APCNs would be interesting for applications, where hydrophobic molecules are to be extracted from an aqueous phase, for instance for removing oil from contaminated water or, alternatively, for slow and controlled release of active agents.[15–17] For such applications, the semisolid nature of gels, enabling their easy mechanical removal after the application, might be very advantageous.

Such a hydrogel of an oil-swollen APCN would then in principle resemble an interconnected micromulsion system, the main difference being that the APCN hydrophobic domains have relatively fixed positions in space with mobility, while microemulsion droplets would be bound, but retaining a certain mobility. Forming networks of microemulsion droplets is possible and has been achieved by adding hydrophobically modified polymers, especially water-soluble polymers, such as polyethylene oxide (PEO), doubly end-capped with hydrophobic segments to microemulsions[18–20]. This can lead to a substantial enhancement of the viscosity, once a percolated network of microemulsion droplets is attained.[21] However, this is a transient network as the hydrophobic stickers in the microemulsion droplets have a defined lifetime, and microemulsion droplets have finite diffusivities. In contrast, an oil-swollen conetwork would differ by the fact that it is a permanent network with immobile hydrophobic nodes.

The oil solubilisation ability of APCNs recently has been addressed theoretically by an analysis of the resulting Gibbs free energies, where the focus was on the relation between solubilisation capacity, its relation to the morphology of the APCN structure, and solubilisation induced structural changes.[22] This work analyses the behaviour of end-linked ABA triblock copolymers with a hydrophilic, ionisable mid-block and hydrophobic non-ionic end-blocks, and found transitions from spheres to cylinders and lamellae as the conetwork hydrophobic content increased and the degree of ionization decreased. These structural transitions go along with discontinuous changes in the degree of swelling and the oil solubilisation abilities.

The combination of the solubilisation properties of amphiphilic systems with the mechanical and rheological properties of APCNs represents an interesting extension of the solubilisation concept, but it has so far, only been little exploited, although the hydrophobic domains immobilised in an aqueous matrix is a novel approach. In an early investigation, the simultaneous swelling of an amphiphilic PEO/PDMS conetwork by a mixture of n-heptane/water was studied, showing an independent swelling of the hydrophilic and of the hydrophobic domains.[23] In a later study on hydrogels based on PEO cross-linked with tris[3-(trimethoxysilyl) propyl] isocyanurate (ICS), it was observed that these gels can be swollen simultaneously by water and toluene, where the extent of swelling depended on the length of

the PEO blocks.[24] A similar study on toluene/water mixtures was also done for star PEG-based amphiphilic copolymers with 1,8 bis(triethoxysilyl) octane as hydrophobic part.[25] However, no systematic study has been done, in which the molecular architecture of the APCN has been varied in a controlled way and in which different types of solubilisates of variable polarity have been employed. Especially, the extent of hydrophobic modification of the APCN is a very interesting parameter to vary and thereby to control the solubilisation properties, something that has never been addressed so far.

Accordingly, filling this gap is the principal aim of our investigation, in which we studied the effect of solubilising oils of different polarity in APCNs based on methyl methacrylate (MMA or M) as hydrophobic and 2-(dimethylamino)ethyl methacrylate (DMAEMA, D) as hydrophilic block, which were cross-linked by ethylene glycol dimethacrylate (EGDMA, E). APCNs of different architecture and different hydrophilic/hydrophobic balance were synthesised, on the basis of DMD or MDM block sequences with constant total length and which vary systematically in the relative proportions of D and M parts. All of them were then swollen with water and one oily compound, for which we chose octane, toluene, eugenol, and 1-hexanol, in order to have a systematic variation of oil polarity. The structure of these oil- and water-swollen APCNs was investigated by means of small-angle neutron scattering (SANS), as this method allows to elucidate structural changes on the nm-scale in such complex systems in good detail. The hydrophobic M part was used in deuterated form, which makes the changes of solubilisation of a hydrogenated oily compound particularly visible in SANS experiments and D2O was used as a solvent for having better contrast and a lower incoherent background. From these investigations, we deduce systematic correlations between the polarity of the oil, the architecture of the copolymer network and how both determine the solubilisation properties of such systems.

Methods and Materials

Materials. The main reagents used for the polymerizations were purchased from Aldrich, Germany. These were 2-(dimethylamino)ethyl methacrylate (D, 98%), deuterated methyl methacrylate (d8-M, 99%), ethylene glycol dimethacrylate (E, 98%), tetrabutylammonium hydroxide (40% w/w in water), benzoic acid (99.5%) and 2,2-diphenyl-1-picrylhydrazyl hydrate (DPPH, 95%). THF was purchased from Labscan, Ireland, and was used as the mobile phase in chromatography (HPLC grade), and as a solvent (reagent grade) for the

polymerizations. Furthermore, 1,4-(dicarcoxylic-dimethylester) cyclohexane, di-isopropylamine, 2.5 M solution of n-butyllithium in hexane, trimethylchlorosilane were used for the sysnthsis of the bifunctional initiator 1,4-bis(methoxytrimethylsiloxymethylene) cyclohexane, MTSMC.

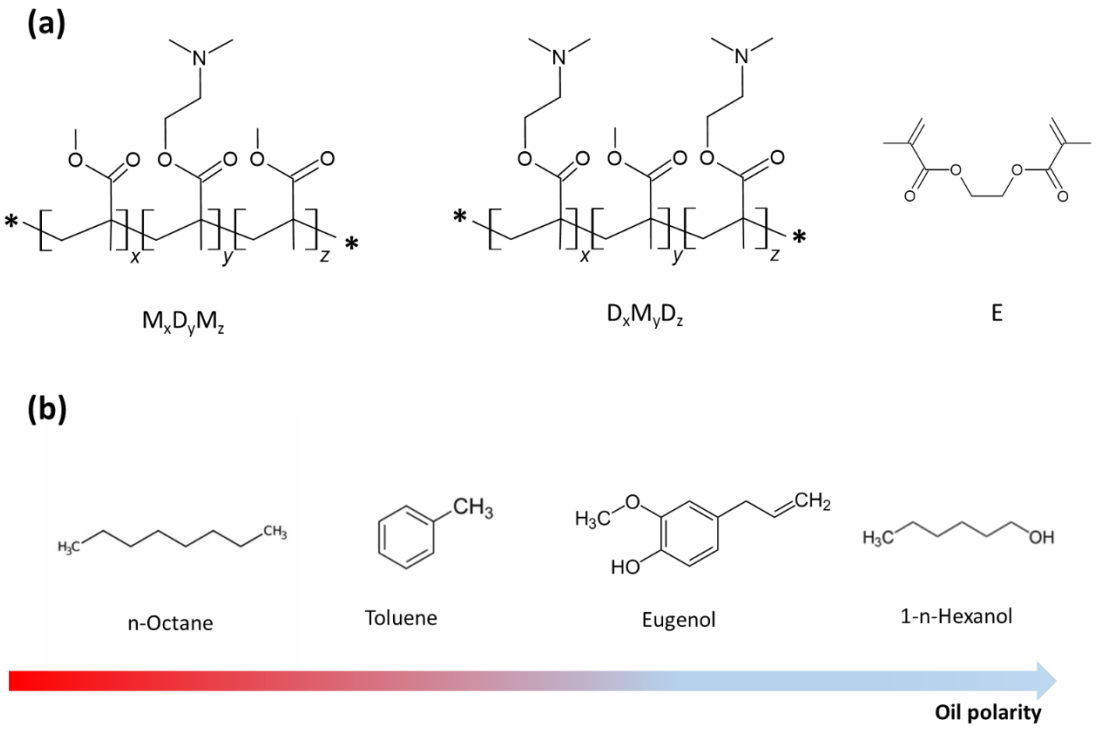

Scheme 1. (a) Chemical structure of the copolymers and the ethylene glycol dimethacrylate (E) crosslinker (b) The oils of different polarity employed in this study. Eugenol is less polar than hexanol according to their dielectric constants.[26] The octanol-water partition coefficients LogP are: octane: LogP = 5.18;[27] toluene: LogP = 2.53; eugenol: LogP = 2.26;[28] 1-n-hexanol: LogP = 2.03.[27] solubility in water: n-octane: 0.66 mg/L (25 °C);[29] toluene: 0.519 g/L (25 °C);[30] eugenol: 2.46 g/L (25 °C);[31] 1-hexanol: 5.9 g/L (25 °C).[32]

As oils of different polarity for the solubilisation experiments, we employed n-octane, toluene, eugenol, and 1-n-hexanol (purchased from Aldrich, Germany), as shown in Scheme 1. Here we also listed two parameters indicative of the polarity of an oil, the octanol-water partition coefficient P, and the solubility in water. These values show that n-octane is very hydrophobic compared to the other compounds. PMMA is also completely insoluble in octane.[33] Toluene and eugenol are close to each other in that respect, but with toluene having somewhat more hydrophobic values. Finally, the 1-n-hexanol is clearly the most hydrophilic oil and with its amphiphilic properties it is also a classical cosurfactant.[34,35] Furthermore, our own studies have

shown that PMMA (Mw: 5 kDa) does not dissolve at all in n-octane and 1-hexanol, but is clearly soluble in toluene and eugenol.

Network Synthesis. Ten polymeric networks based on amphiphilic triblock copolymers composed of deuterated MMA and hydrogenated DMAEMA were synthesized (see Table 1). The synthesis was carried out with the use of a bifunctional initiator (MTSMs) in a three-step procedure. The total degree of polymerization was 40 in all cases (Table 1), covering two different architectures, MDM and DMD triblock copolymers, and five different compositions (d_8-MMA:DMAEMA) 10:90, 30:70, 50:50, 70:30, and 90:10. As an example, the polymerization procedure followed for the synthesis of the APCN with the structure EGDMA$_4$-DMAEMA$_{10}$-*b*-d_8-MMA$_{20}$-*b*-DMAEMA$_{10}$-EGDMA$_4$ is described in this paragraph. Freshly distilled THF (23 mL) and 0.3 mL bifunctional initiator MTSMC (0.36 g, 1.05 mmol) were transferred via glass syringes, in this order, to a 100-mL round-bottomed flask containing a small amount (~10 mg) of TBABB catalyst, sealed with a rubber septum and kept under a dry nitrogen atmosphere. This was followed by the slow addition of 2.2 mL of d_8-MMA (2.2 g, 20.8 mmol) under stirring. The polymerization exotherm (23.2-39.3 ^{o}C) abated within 5 minutes, resulting in the linear homopolymer d_8-MMA$_{20}$. Next, 3.5 mL of DMAEMA (3.3 g, 20.9 mmol) were added under stirring. The polymerization exotherm (31.6-43.1 ^{o}C) abated within 5 minutes, resulting in the linear triblock copolymer DMAEMA$_{10}$-*b*-d_8-MMA$_{20}$-*b*-DMAEMA$_{10}$. In the third and final stage, 1.6 mL (1.7 g, 8.37 mmol) of the EGDMA cross-linker was added, which promoted the gelation of the solution within 2 minutes, and caused a temperature increase from 32.5 to 38.2 ^{o}C. The network synthesis was done in THF which is a good solvent for all monomers. The syntheses of the remaining APCNs were done in the same way but using different amounts of MMA or DMAEMA as well as reverting the order of addition of MMA and DMAEMA. The molecular weights determined by gel permeation chromatography with refractive index detection (and poly(methyl methacrylate) standard calibration) of the middle blocks and the triblock copolymers are listed in Table 1.

Table 1. Molecular weights of deuterated linear triblock copolymers determined using GPC.

No.	Polymer Structure	Molecular weights by GPC-RI			
		M_{theory}	M_p	M_n	M_w/M_n
1	MMA(d_8)$_4$	433	1010	851	1.27
	DMAEMA$_{18}$-*b*-MMA(d_8)$_4$-*b*-DMAEMA$_{18}$	6093	8190	8980	1.19
2	MMA(d_8)$_{12}$	1298	2580	2380	1.24
	DMAEMA$_{14}$-*b*-MMA(d_8)$_{12}$-*b*-DMAEMA$_{14}$	5700	7460	8200	1.18
3	MMA(d_8)$_{20}$	2163	5290	3740	1.21
	DMAEMA$_{10}$-*b*-MMA(d_8)$_{20}$-*b*-DMAEMA$_{10}$	5307	11500	8250	1.18

4	MMA(d_8)$_{28}$	3029	7010	5530	1.14
	DMAEMA$_6$-*b*-MMA(d_8)$_{28}$-*b*-DMAEMA$_6$	4915	10500	8370	1.16
5	MMA(d_8)$_{36}$	3894	7460	6100	1.13
	DMAEMA$_2$-*b*-MMA(d_8)$_{36}$-*b*-DMAEMA$_2$	4523	8720	7140	1.14
6	DMAEMA$_{36}$	5660	11900	9680	1.15
	MMA(d_8)$_2$-*b*-DMAEMA$_{36}$-*b*-MMA(d_8)$_2$	6093	13500	10900	1.17
7	DMAEMA$_{28}$	4402	5630	6200	1.17
	MMA(d_8)$_6$-*b*-DMAEMA$_{28}$-*b*-MMA(d_8)$_6$	5700	7230	7820	1.18
8	DMAEMA$_{20}$	3144	5130	5160	1.16
	MMA(d_8)$_{10}$-*b*-DMAEMA$_{20}$-*b*-MMA(d_8)$_{10}$	5307	7940	8340	1.18
9	DMAEMA$_{12}$	1887	4670	3480	1.21
	MMA(d_8)$_{14}$-*b*-DMAEMA$_{12}$-*b*-MMA(d_8)$_{14}$	4915	11200	8700	1.14
10	DMAEMA$_4$	629	1430	1180	1.31
	MMA(d_8)$_{18}$-*b*-DMAEMA$_4$-*b*-MMA(d_8)$_{18}$	4523	8720	6920	1.15

Characterization of the Degree of Swelling (DS) of the Networks. The degrees of swelling (DSs) of all the conetworks were measured in pure water, in aqueous solutions of various pH covering the range between 2 and 11, and also in THF. The DS were calculated as the ratio of the mass of the swollen gel divided by that of the dry conetwork. All masses were determined gravimetrically. All aqueous DS were determined in triplicate and the averages of the measurements together with their standard deviation are presented in the Table 2 for the THF, low pH (2-3.5) water and high pH (9-11) water.

Table 2: Degree of swelling in THF, low pH (2-3.5), and high pH (9-11) water for the different polymer conetworks

No.	**Polymer conetwork structure**	**Degree of Swelling**		
		THF	**Low pH**	**High pH**
1	MMA(d_8)$_{18}$-*b*-DMAEMA$_4$-*b*-MMA(d_8)$_{18}$	3.7 ± 0.5	2.3 ± 0.3	2.0 ± 0.4
2	MMA(d_8)$_{14}$-*b*-DMAEMA$_{12}$-*b*-MMA(d_8)$_{14}$	3.5 ± 0.4	3.1 ± 0.4	1.8 ± 0.1
3	MMA(d_8)$_{10}$-*b*-DMAEMA$_{20}$-*b*-MMA(d_8)$_{10}$	4.0 ± 0.4	8.8 ± 0.9	2.0 ± 0.3
4	MMA(d_8)$_6$-*b*-DMAEMA$_{28}$-*b*-MMA(d_8)$_6$	4.4 ± 0.8	14.7 ± 2.3	3.0 ± 0.2
5	MMA(d_8)$_2$-*b*-DMAEMA$_{36}$-*b*-MMA(d_8)$_2$	4.8 ± 0.4	20.0 ± 1.7	3.3 ± 0.6
6	DMAEMA$_{18}$-*b*-MMA(d_8)$_4$-*b*-DMAEMA$_{18}$	4.7 ± 0.2	17.5 ± 1.7	3.5 ± 0.2
7	DMAEMA$_{14}$-*b*-MMA(d_8)$_{12}$-*b*-DMAEMA$_{14}$	4.2 ± 0.4	11.8 ± 0.7	2.6 ± 0.4
8	DMAEMA$_{10}$-*b*-MMA(d_8)$_{20}$-*b*-DMAEMA$_{10}$	4.0 ± 0.5	10.4 ± 1.1	1.7 ± 0.1
9	DMAEMA$_6$-*b*-MMA(d_8)$_{28}$-*b*-DMAEMA$_6$	3.8 ± 0.1	3.1 ± 0.4	1.9 ± 0.1
10	DMAEMA$_2$-*b*-MMA(d_8)$_{36}$-*b*-DMAEMA$_2$	3.5 ± 0.5	2.5 ± 0.5	1.7 ± 0.2

The hydrophilic DMAEMA block is ionisable and is therefore charged at low pH and neutral at high pH. DMAEMA copolymer has a pK_A of 7.8,[36] meaning that at neutral pH (that of D_2O added for the SANS experiments), the polymer is only slightly ionized. The results of the swelling experiments given in Table 1 show that the degree of swelling in the common solvent THF is rather similar for all conetworks studied. In water at high pH, the swelling varies only

little with the copolymer composition, and is much smaller than in THF, but clearly correlates well with the length of the hydrophilic DMAEMA block. This correlation is retained at low pH, but here the relative changes are much more pronounced and values of up to 20 for the degree of swelling are observed for the longest DMAEMA blocks, due to electrostatic repulsion among charged DMAEMA blocks. Interestingly, the copolymer architecture (MDM vs. DMD) has only a small effect on the absolute values of the degree of swelling.

Small-angle neutron scattering (SANS)

The SANS experiments were performed at the instrument PAXE of the Laboratoire Léon Brillouin (LLB) equipped with a 64x64 pixel detector, using a wavelength of λ=6 Å ($\Delta\lambda$ = 10%) and two sample-to-detector distances of 1.2 and 4 m, thereby covering a q-range of 0.07-3.1 nm^{-1}. Samples were loaded into 1 mm thick quartz cells. The 2D-detector data were reduced and normalized by an incoherent scatterer (plexiglass) to correct the detector cell efficiency, corrected for electronic background, subtracted the scattering of the empty cell and radially averaged using the BerSANS software.[37] All the data were normalised to absolute scale.
The incoherent background arising mainly from the hydrogens in the polymer as well as the oils, was not subtracted from the data.

The SANS experiments were done with fifty samples of polymer networks with ten different copolymer compositions, swollen in neat deuterated water. Forty of the samples had been pre-swollen in four organic oils (n-octane, eugenol, toluene, n-1-hexanol) before being swollen in D_2O, whereas the remaining ten samples were directly swollen in D_2O.

The SANS curves were mainly analysed in structural terms by determining the position of the maxima q_{max} from Kratky type plots of $I(q)q^2$ vs. q (see Figure 2b and SI). All the measurements were carried out at room temperature.

Results and Discussion

In our experiments, we focused on the structural changes occurring in different APCNs swollen in water upon the solubilisation of various oils of different polarity (done such that the APCNs can be expected to be saturated with the oil and in an equilibrated state). The mesoscopic structure was determined by means of small-angle neutron scattering (SANS), accessing detailed structural information in the relevant size range of 0.5-100 nm. In order to have good contrast conditions, all these experiments were done in D_2O solvent and using hydrogenated oils. To highlight the solubilisation of hydrogenated oils, the DMAEMA and EGDMA repeat units of the amphiphilic polymers were hydrogenated and the MMA monomers deuterated.

Thus, due to the use of deuterated hydrophobic monomer MMA, the scattering contrast conditions are modified by the fact that the hydrophobic (d-MMA) and hydrophilic parts (DMAEMA swollen with D_2O) have relatively high scattering length densities (SLDs) that are rather close in value. However, its advantage is that for this contrast condition the solubilisation of a hydrogenated oil has a large impact on the SLD of the hydrophobic part and therefore this contrast condition is rather sensitive to the solubilisation effects studied by us. The contrast conditions relevant to this system are depicted in Figure 1, indicating the effect of swelling of DMAEMA by D_2O, of the content of the EGDMA cross-linker on the MMA block (dotted vertical lines), and the values for the different pure oils (that also differ, depending on whether they contain an aromatic moiety or not). One clearly observes in Figure 1 that the swelling of the DMAEMA moves the SLD to larger values, which means that, in these water-swollen APCNs, the addition of an oil has a major impact on the contrast and will easily be identified in the change of the scattering pattern.

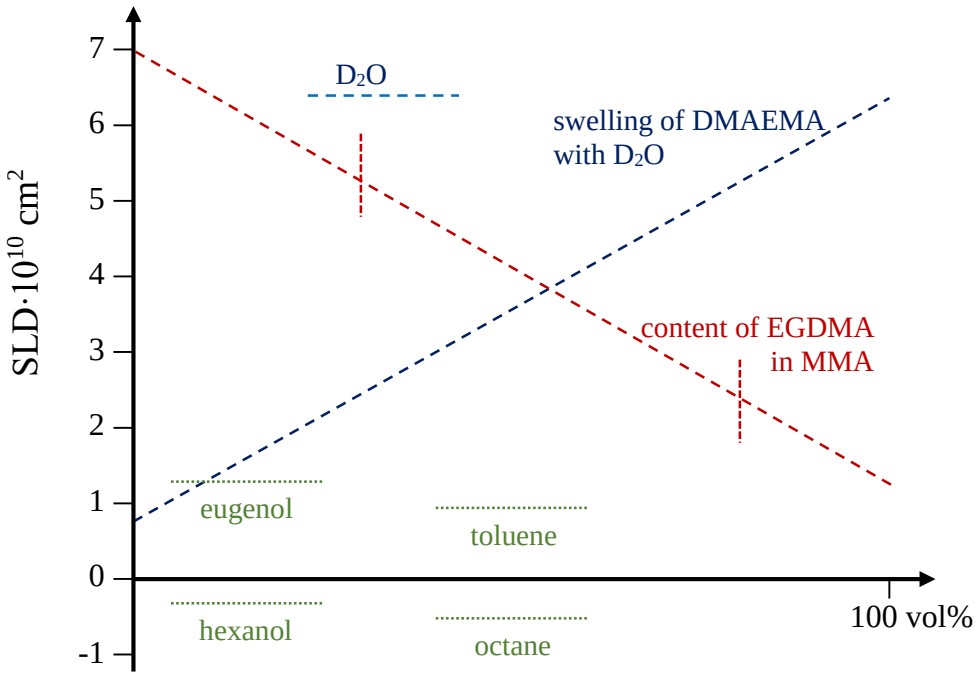

Figure 1. Scattering length densities (SLDs) of the different components contained in the swollen APCNs as a function of the volume fraction in the mixtures. Indicated is how the SLD of the solvated DMAEMA block is changed upon swelling by D_2O, how the SLD of the d_8-MMA changes upon the incorporation of EGDMA (the limits for the different copolymers employed are indicated), and the SLDs of the 4 different oils employed and that of D_2O.

Polymer Conetworks Swollen in D_2O

In a first step, we looked at the binary system of APCNs swollen with excess D_2O, whose SANS curves are given in Figure 2. The scattering curves are characterized by three distinct features from high to low q-range. At high q the contributions of the incoherent scattering and the scattering of the polymer chains results in a moderate intensity decrease with q. At intermediate q, the slope becomes steeper close the q^{-4} indicative of spherical objects, this feature being much variably pronounced, depending on the type of copolymer and also on the type of oil solubilised. At lower q, all of them show a correlation peak (or at least an indication for it). This confirms that in all cases marked micro-phase separation takes place, leading to ordered hydrophobic domains, and this even for the shortest D_4 block, as demonstrated by the correlation peak at $q \sim 1.1$ nm^{-1}, indicating a domain spacing of ~ 5 nm. Interestingly, this structuring is similarly pronounced for the D_{12} block, but with a smaller spacing, and almost vanishes for the D_{20} and D_{28} block, while the scattering intensity increases, thereby indicating the formation of larger hydrophobic and less ordered domains. In contrast, the hydrogel with the longest, D_{36} block (APCN no. 5) shows again a clear correlation peak, but at $q \sim 0.4$ nm^{-1}, meaning that here the spacing is about 15 nm. In general, the degree of ordering of the hydrophobic domains is higher for the APCNs with a central MMA (M) block than for a central DMAEMA (D) block. The generally lower scattering intensity for the samples with central D block may be explained by the fact that the hydrogenated E_4 block automatically well incorporates within the hydrophobic M domain, thereby leading to a reduction of its SLD (see Figure 1).

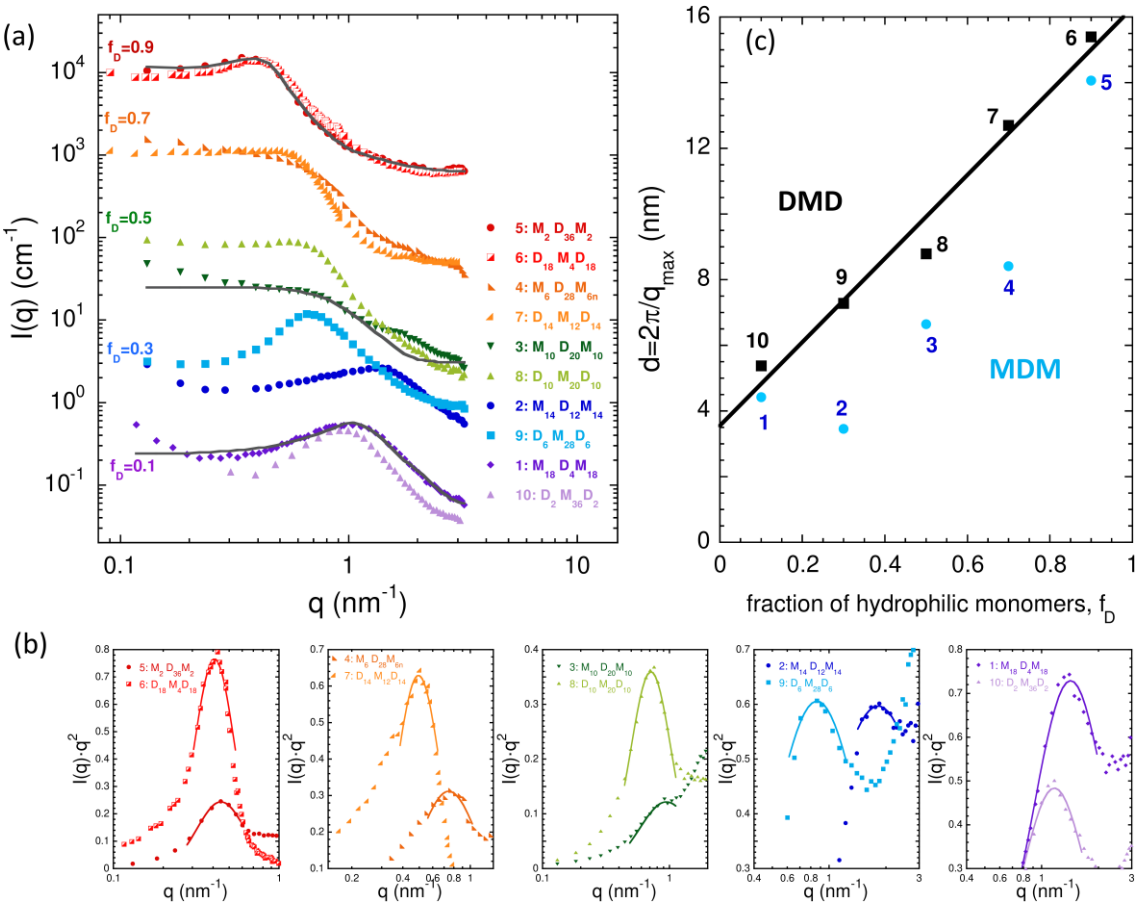

Figure 2. **(a)** SANS curves for the different APCNs swollen in D_2O. Subsequent pairs of curves were multiplied by a factor 10^n, for better distinction of curves; Solid lines are fits to a model of polydisperse spheres described in ref.[38] **(b)** Kratky-Porod plot, $I(q)q^2$, of the same data, showing better the peak position of the respective data sets. Solid lines are fits to a Gaussian function (see SI) **(c)** the mean spacing d, as calculated from the peak position q_{max} via $d = 2\pi/q_{max}$. The solid line is a guide to the eye. The legends indicate the APCN number (see Table 2) and copolymer structure $M_xD_yM_x$ where x and y indicate the polymerization degree of the MMA (M) and DMAEMA (D) blocks, respectively.

Generally, the scattering curves of such networks with microphase separation are often interpreted in terms of a sum of two contributions: (1) A contribution of the polymer chains (generally an Ornstein-Zernike term), and (2) a contribution of polydisperse homogeneous spheres formfactor with a hard sphere structure factor.[38] This model fit works well for the networks in D_2O with low and high D monomer content (see Figure 2a). In the case of $M_{18}D_4M_{18}$, we find a sphere radius of R =1.2 nm and a hard sphere radius of R_{HS} = 2.6 nm; and in the case of $M_2D_{36}M_2$ the size is R = 4.1 nm and R_{HS} = 7.0 nm. However, this system is neither comprised of homogeneous spheres nor is it a hard sphere system. The model just

provides an effective size of the domains as well as a correlation length. Note, that the correlation length between domains obtained from the hard sphere size compares very well to the distance obtained from the peak maxima. Moreover, this simplified model fails in the case of intermediate hydrophilic content and the structure can no longer be described as a sphere, see e.g., the case of $M_{10}D_{20}M_{10}$ in Figure 2a. Thus, to compare all the different networks the best analysis is in terms of the size of the domains obtained through the correlation peak.

In order to precisely quantify the peak position q_{max}, we used the Kratky representation; i.e. plots of $I(q)q^2$ vs. q, where the maximum is better defined, as it reduces effects of the form factor on the peak position (see Figure 2b). We also verified that the uncertainty regarding the precise value of the background has an effect of less 4% on the deduce value of q_{max}, for the more marked peaks much less. From q_{max} the mean spacing between the hydrophobic domains was estimated as $d\ (= 2\pi/q_{max})$. Figure 2c shows a systematic correlation with the composition of the APCN: the mean spacing d correlates directly with the D content in the APCNs (f_D is the mol fraction compared to the M units). As shown in Figure 2c, we observe a linear relation of d with the percentage of D content, which means that the length of the swollen D block determines the spacing in the swollen APCN. However, while this relation is very well fulfilled for the samples APCNs no. 6-10 with the central M block, the swelling with increasing length of the D block is less pronounced for APCNs no. 1-5 with the central D block at intermediate values of f_D, leading to almost identical values for highest and lowest D content. This means that the structural distance of the hydrophobic domains in the ordered hydrogels is not affected by the size of the hydrophobic domains themselves (which should be related to the length of the M block). This might be explained by the fact that the EGDMA placed in the centre of the linking D block has a weaker tendency for extension and may partly lead to D chains being tethered to hydrophobic domains again. In general, it is not surprising that similar spacings irrespective of the architecture (central D or M block) are observed as the central M-block has half the length of the D-block. Actually, the connection occurs via a D_n-E_4-D_n unit, which has about the same total D length and apparently the presence of the E_4 block has no major effect here. From the slope of the spacing shown in Figure 2c, one may conclude that one D unit contributes by 0.3 nm to the mean spacing d, which means that the hydrophobic domains must be connected by almost fully stretched D blocks (as the stretched length per monomer is 0.25 nm). The linear relationship itself already indicates that no coiling of the hydrophilic block has yet an effect on d. The intercept of ~3.5 nm for zero D content indicates a minimum structural size of domains given by the M and E parts of the APCNs.

Oil Solubilisation in Aqueous Polymer Conetworks

After having characterised the pure aqueous APCN systems, in the next step we investigated the structural changes taking place upon solubilisation of oils of different polarity. The aqueous hydrogels were equilibrated in the corresponding oil (for details see the experimental section). In Figure 3, we show two examples of the APCNs, D_6-M_{28}-D_6 and M_{10}-D_{20}-M_{10}, that were swollen in water and then, in water and in the presence of one of the studied oils (the complete set of scattering curves for a given APCN and swollen with the different oils is shown in Figure S1). First, looking at the most hydrophobic oil, octane, we observe that its addition has basically no effect on the structures observed by SANS, as shown in Figures S1 and S4, that displayed scattering curves almost identical to those without added octane. This indicates that the aliphatic hydrocarbon octane does not become solubilised at all. In contrast, the addition of the other oils (toluene, eugenol, and 1-hexanol) leads to marked changes in the scattering patterns. The presence of toluene results in a substantial increase in the small angle scattering intensity, where this effect is less pronounced for M_2-D_{36}-M_2 and D_{18}-M_4-D_{18} (Figure S1i and S1j). Apparently, there, the hydrophobic domains are too small to become swollen to a larger extent and, consequently, could not incorporate larger amounts of toluene, compared to the network swollen only in D_2O. The addition of 1-hexanol generally leads to similar scattering patterns at higher q-values as toluene addition. However, at low q one typically sees a larger intensity upturn for 1-hexanol which is not seen for toluene. Finally, the scattering patterns of samples with eugenol look similar to the ones with hexanol, but especially for short M blocks, a more erratic development of scattering patterns is observed (see Figure S1). For instance, for M_2-D_{36}-M_2 (Figure S1i) very large and unordered structures are seen, while for M_6-D_{28}-M_6 (Figure S1d) rather small and ordered structures are present.

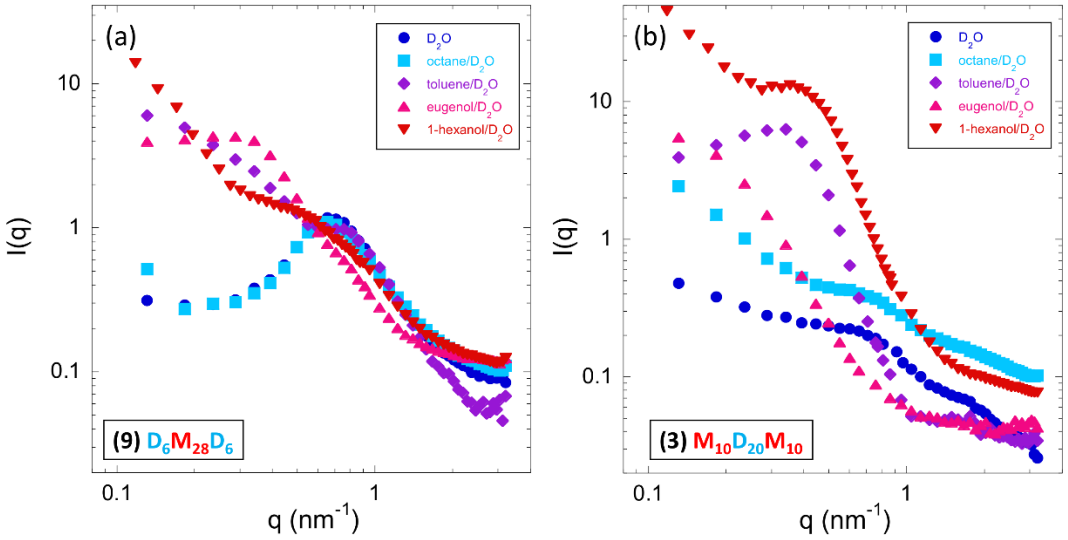

Figure 3. SANS curves of the APCNs D_6-M_{28}-D_6 (a) and M_{10}-D_{20}-M_{10} (b) swollen in D_2O and saturated with octane, toluene, eugenol, and 1-hexanol.

Looking now in more detail to the effect of the different added oils, we find that the polar aromatic hydrocarbon toluene leads to the most pronounced changes of the scattering patterns (Figure 4a). Already for the shortest D_4-block, one sees a marked shift of the correlation peak to lower q and a substantial increase in intensity, which indicates the formation of much larger hydrophobic domains in the system, i.e., the M domains must have been swollen largely (here it should be noted that PMMA is fully miscible with toluene[33]). For the D_{12}-system, this effect is even more pronounced and here also the correlation peak is sharper, indicating a more extended ordered structure. The ordering effect is still present for the D_{20}-system, but vanishes largely for the D_{28}-system, while much larger aggregates are formed compared to the system in pure water. However, for the longest D_{36}-block, toluene addition has almost no effect on the size and ordering of the formed aggregates and apparently the M/EGDMA block is too small to facilitate any larger toluene solubilisation.

It is very interesting to point out that the mean spacing d of the different samples, which is basically constant within the experimental uncertainties (Figure 4b) and no longer correlates with the D monomer content (only APCN no. 4 is deviating here, without obvious explanation). Its mean value of ~15 nm corresponds to the maximum d of the pure polymer conetworks, as shown in Figure 2. The logical explanation might be that the M block is fully swollen, like the D block by D_2O. Accordingly, if both blocks are fully swollen in a respective good solvent, the spacing should just be determined by the total length of the blocks between the cross-linking points and this is a constant in the polymers studied here.

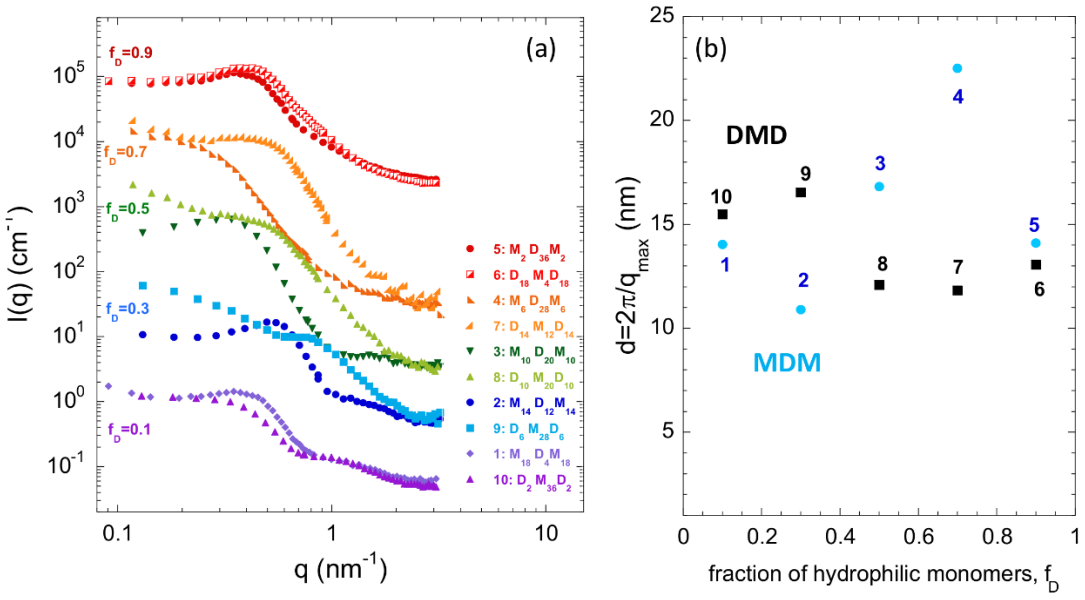

Figure 4. **(a)** SANS curves for the different APCNs swollen simultaneously in D_2O and toluene (for clarification subsequent data pairs were shifted upwards by multiplying with a factor 10); **(b)** the mean spacing d, as calculated from the peak position q_{max} via $d = 2\pi/q_{max}$. The legends indicate the APCN number (see Table 2) and copolymer structure $M_xD_yM_x$ where x and y indicate the polymerization degree of the MMA (M) and DMAEMA (D) blocks, respectively.

The very polar oil 1-hexanol, which actually is a typical cosurfactant[39,40] and surface active, leads also to a loss of structural ordering for the shortest D_4 block, but for longer D-blocks one can see an increased scattering intensity and the formation of larger hydrophobic domains (Figure 5 left). 1-Hexanol apparently contributes to micro-phase separation and the formation of larger domains. In general, the scattering curves show some resemblance to those with toluene (Figure 4a), but differ mostly with respect to a much more marked upturn at lower q. This may indicate the formation of a network between the ordered domains. Hexanol may both facilitate its formation but also makes it more visible by attaching to the polymer chains forming it, due its amphiphilic character.

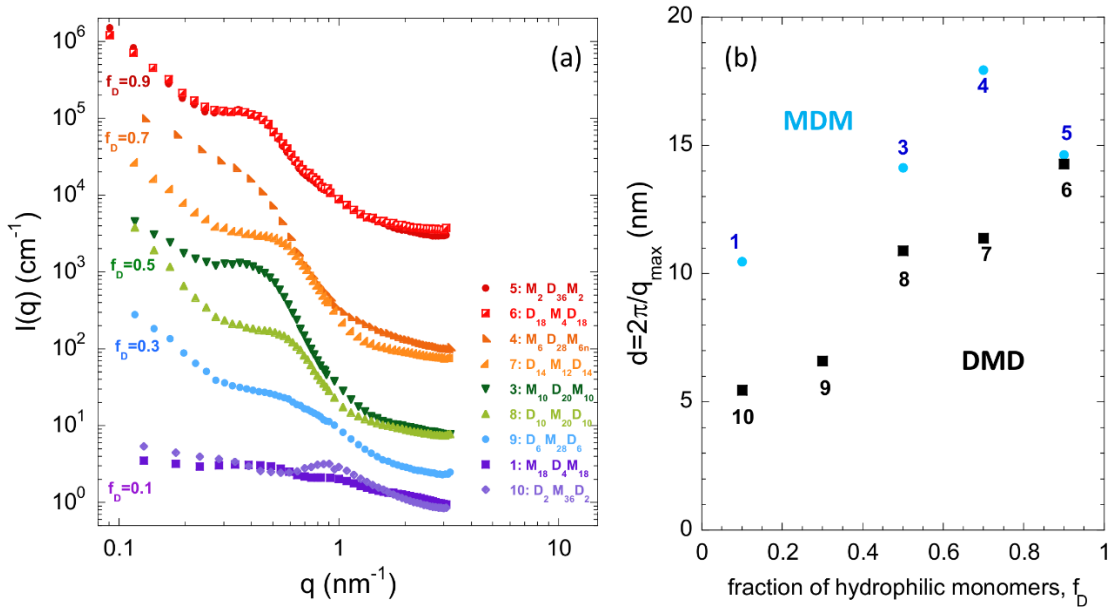

Figure 5. (a) SANS curves for the different APCNs swollen simultaneously in D_2O and 1-hexanol (for clarification subsequent data pairs were shifted upwards by multiplying with a factor 10). The legends indicate the APCN number (see Table 2) and copolymer structure $M_xD_yM_z$ where x,y and z indicate the polymerization degree of the MMA (M) and DMAEMA (D) blocks. **(b)** The mean spacing d, as calculated from the peak position q_{max} via $d = 2\pi/q_{max}$.

Looking at the spacing d (Figure 5a), one finds an intermediate behavior between the pure polymers and the ones completely swollen by toluene, i.e. one observes a substantial swelling for low D content but the relative extent of additional swelling becomes smaller with increasing D block length. It is very interesting to note that the spacing now is always much larger for the APCNs with D block in the centre (APCN no. 6-10). A logical explanation would be that the swelling of the M block is easier when the E_4 block is also present in the hydrophobic domain, than without it. It may also indicate that the hexanol interacts more strongly with the D block and leads to a swelling and stretching of the D chains. Clearly different is the situation for low values of f_D, where for toluene large swelling is seen, while for 1-hexanol almost no swelling is seen when the long M block is in the middle (APCN no.10) and d is about the same as for the APCN in pure D_2O (Figure 2b). For having the same f_D copolymer with the M blocks next to the EGDMA core, the value is about twice, with 10 nm. Obviously, 1-hexanol is very selective with respect to its solubilisation properties and not much associating with the M domains. An explanation could be that 1-hexanol is simply too amphiphilic and prefers to reside

at the amphiphilic interface or interact strongly with the D but does not much become incorporated into the M domains.

For eugenol, it should first be noted that its pK_a at 25 °C is 10.19 [41] and therefore under our experimental conditions it can safely be assumed to be a neutral compound, like the other oils used. Very interestingly, the addition of the rather polar aromatic oil eugenol leads to a disappearance of the correlation peaks and accordingly the degree of ordering in these samples is much reduced. However, the detailed behaviour depends strongly on the type of APCN. For the case of central D-blocks (APCN no. 6-10) the scattering intensity remains generally low, except for M_2-D_{36}-M_2 and to a lesser extent for M_{10}-D_{20}-M_{10}, where a marked increase of scattering intensity towards low q is seen, which could indicate the formation of larger emulsion droplets or elongated structures. For the case of central M-blocks (APCN no. 1-5), the situation is similar for D_{10}-M_{20}-D_{10} and to a lesser extent for D_{14}-M_{12}-D_{14}. Apparently, eugenol is interacting with the aqueous APCN systems such that it suppresses micro-phase separation and ordering to a larger extent. However, for some APCNs it looks like they have a suitable amphiphilic structure to stabilise larger emulsion droplets, which is not seen similarly for the addition of the other oils.

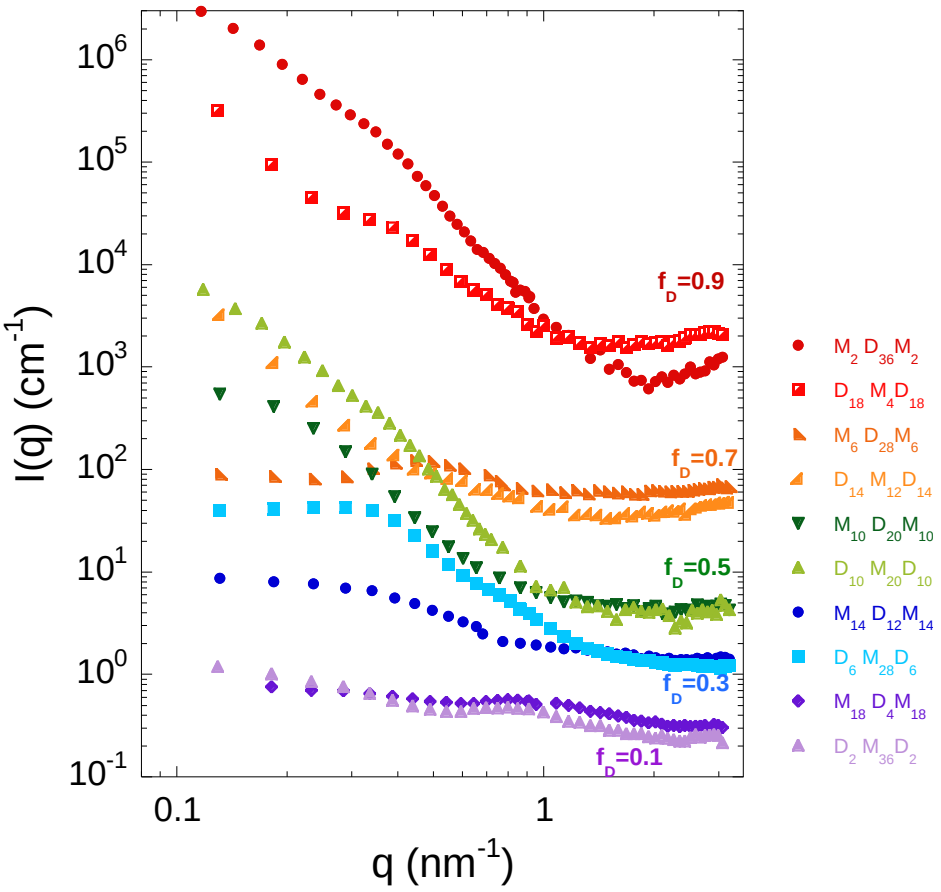

Figure 6. SANS curves for the different APCNs swollen simultaneously in D_2O and eugenol (for clarification subsequent data pairs were shifted upwards by multiplying with a factor 10). The legends indicate the APCN number (see Table 2) and copolymer structure $M_xD_yM_z$ where x, y and z indicate the polymerization degree of the MMA (M) and DMAEMA (D) blocks.

Conclusions

In this study, the oil-swelling behaviour of APCN hydrogels composed of hydrophobic M and hydrophilic D blocks cross-linked by EGDMA was investigated for the solubilisation of oils of different polarity (octane, toluene, eugenol, 1-hexanol). The APCNs were systematically varied with respect to their content of the M and D blocks, while keeping the total length of the connecting arms constant. In addition, we also varied the network architecture by changing which of the two blocks is in the centre of the cross-linked polymeric building blocks. SANS experiments on APCNs swollen by D_2O show that the formed hydrophobic domains have a mean spacing that follows directly the amount of hydrophilic D chains in the APCNs, confirming that their swelling determines the structural arrangement of the hydrophobic

domains. In addition, it is interesting to note that these hydrophobic domains are sufficiently ordered to yield a marked correlation peak in the scattering curves.

The solubilisation experiments, in which the different water-swollen APCNs were saturated with the different oils showed a marked dependence on the polarity of the chosen oil. The most unpolar oil, octane, was basically not solubilised at all, leading to no structural change. In contrast, the more polar oils toluene and 1-hexanol lead to a substantial increase in the spacing and a corresponding increase in the scattering intensity, thereby confirming that both oils become incorporated within the hydrophobic M domains of the APCN hydrogel. However, toluene can become incorporated generally well into the M domains, thereby swelling them and forming a much extended and maximum swollen APCN. In contrast, 1-hexanol swells for medium and low M content similarly, but not for very high M content. This can be explained such that it is more surface active and therefore preferentially resides at the amphiphilic interface. Thus, its contribution to swelling is rather low for high M content. In addition, 1-hexanol appears to be interacting with the D chains and thereby enhances and highlights the presence of an interconnecting network. Finally, the also rather polar oil eugenol shows a more complicated behaviour. With increasing content of the hydrophilic D, it discriminates increasingly the two different APCN topologies. It becomes much more solubilised for the case where M forms the cross-linking cores together with EGDMA. However, here it appears that this solubilisation does no longer occur in the form of becoming solubilised within the hydrophobic core, but instead forming nanoemulsion droplets that become stabilised by the rather small hydrophobic domains.

To conclude, these APCNs are not only interesting novel systems of fundamental interest, but also of high potential for prospective applications where one wants to combine the properties of a polymer gel with the ability to absorb or deliver hydrophobic substances. The D/M system studied here clearly shows a high selectivity in its solubilisation response towards oils of different polarity. This renders this type of APCNs interesting systems for selective solubilisation of different types of oils and also using such hydrogels for selective release applications.

Acknowledgements

We would like to thank Dr. Raphael Michel for help with performing the SANS experiments. The LLB is thanked for granting SANS beamtime for these experiments.

References

(1) Gradzielski, M.; Duvail, M.; de Molina, P. M.; Simon, M.; Talmon, Y.; Zemb, T. Using Microemulsions: Formulation Based on Knowledge of Their Mesostructure. *Chem Rev* **2021**, *121* (10), 5671–5740.

(2) Walstra, P.; Smulders, P. E. A. Emulsion Formation. *Modern aspects of emulsion science* **1998**, 56–99.

(3) Romet-Lemonne, G.; Daillant, J.; Guenoun, P.; Yang, J.; Holley, D. W.; Mays, J. W. Oil-in-Water Microemulsions Stabilized by Charged Diblock Copolymers. *J Chem Phys* **2005**, *122* (6), 064703.

(4) Hurter, P. N.; Scheutjens, J. M. H. M.; Hatton, T. A. Molecular Modeling of Micelle Formation and Solubilization in Block Copolymer Micelles. 1. A Self-Consistent Mean-Field Lattice Theory. *Macromolecules* **1993**, *26* (21), 5592–5601. https://doi.org/10.1021/ma00073a010.

(5) Nagarajan, R.; Barry, M.; Ruckenstein, E. Unusual Selectivity in Solubilization by Block Copolymer Micelles. *Langmuir* **1986**, *2* (2), 210–215. https://doi.org/10.1021/la00068a017.

(6) Nagarajan, R.; Ganesh, K. Solubilization in Spherical Block Copolymer Micelles: Scaling Analysis Based on Star Model. *J Chem Phys* **1993**, *98* (9), 7440–7450. https://doi.org/10.1063/1.464708.

(7) Hurter, P. N.; Hatton, T. A. Solubilization of Polycyclic Aromatic Hydrocarbons by Poly(Ethylene Oxide-Propylene Oxide) Block Copolymer Micelles: Effects of Polymer Structure. *Langmuir* **1992**, *8* (5), 1291–1299.

(8) Kwon, G. S.; Forrest, M. L. Amphiphilic Block Copolymer Micelles for Nanoscale Drug Delivery. *Drug Dev Res* **2006**, *67* (1), 15–22. https://doi.org/10.1002/ddr.20063.

(9) Kafouris, D.; Gradzielski, M.; Patrickios, C. S. Semisegmented Amphiphilic Polymer Conetworks: Synthesis and Characterization. *Macromolecules* **2009**, *42* (8), 2972–2980.

(10) Kepola, E. J.; Loizou, E.; Patrickios, C. S.; Leontidis, E.; Voutouri, C.; Stylianopoulos, T.; Schweins, R.; Gradzielski, M.; Krumm, C.; Tiller, J. C.; Kushnir, M.; Wesdemiotis, C. Amphiphilic Polymer Conetworks Based on End-Linked "Core-First" Star Block Copolymers: Structure Formation with Long-Range Order. *ACS Macro Lett* **2015**, *4* (10), 1163–1168.

(11) Kepola, E. J.; Kyriacou, K.; Patrickios, C. S.; Simon, M.; Gradzielski, M.; Kushnir, M.; Wesdemiotis, C. Amphiphilic Polymer Conetworks Based on Interconnected Hydrophobic Star Block Copolymers: Synthesis and Characterization. *Macromol Symp* **2017**, *372* (1), 69–86.

(12) Patrickios, C. S.; Matyjaszewski, K. Amphiphilic Polymer Co-networks: 32 Years Old and Growing Stronger – a Perspective. *Polym Int* **2021**, *70* (1), 10–13.

(13) Triftaridou, A. I.; Hadjiyannakou, S. C.; Vamvakaki, M.; Patrickios, C. S. Synthesis, Characterization, and Modeling of Cationic Amphiphilic Model Hydrogels: Effects of Polymer Composition and Architecture. *Macromolecules* **2002**, *35* (7), 2506–2513. https://doi.org/10.1021/ma0114077.

(14) Vamvakaki, M.; Patrickios, C. S.; Lindner, P.; Gradzielski, M. Amphiphilic Networks Based on Cross-Linked Star Polymers: A Small-Angle Neutron Scattering Study. *Langmuir* **2007**, *23* (21), 10433–10437.

(15) Hurter, P. N.; Hatton, T. A. Solubilization of Polycyclic Aromatic Hydrocarbons by Poly(Ethylene Oxide-Propylene Oxide) Block Copolymer Micelles: Effects of Polymer Structure. *Langmuir* **1992**, *8* (5), 1291–1299.

(16) Kim, J.-Y.; Cohen, C.; Shuler, M. L.; Lion, L. W. Use of Amphiphilic Polymer Particles for In Situ Extraction of Sorbed Phenanthrene from a Contaminated Aquifer Material. *Environ Sci Technol* **2000**, *34* (19), 4133–4139.
(17) Ghasdian, N.; Church, E.; Cottam, A. P.; Hornsby, K.; Leung, M.-Y.; Georgiou, T. K. Novel "Core-First" Star-Based Quasi-Model Amphiphilic Polymer Networks. *RSC Adv* **2013**, *3* (41), 19070.
(18) Gradzielski, M.; Rauscher, A.; Hoffmann, H. Hydrophobically Cross-Linked Micellar Solutions : Microstructure and Properties of the Solutions. *Journal de Physique IV* **1993**, *03* (C1), C1-65-C1-79.
(19) Michel, E.; Filali, M.; Aznar, R.; Porte, G.; Appell, J. Percolation in a Model Transient Network: Rheology and Dynamic Light Scattering. *Langmuir* **2000**, *16* (23), 8702–8711.
(20) Malo De Molina, P.; Herfurth, C.; Laschewsky, A.; Gradzielski, M. Structure and Dynamics of Networks in Mixtures of Hydrophobically Modified Telechelic Multiarm Polymers and Oil in Water Microemulsions. *Langmuir* **2012**, *28* (45), 15994–16006.
(21) Malo de Molina, P.; Appavou, M.-S.; Gradzielski, M. Oil-in-Water Microemulsion Droplets of TDMAO/Decane Interconnected by the Telechelic C_{18}-EO_{150}-C_{18}: Clustering and Network Formation. *Soft Matter* **2014**, *10* (28), 5072–5084.
(22) Varnava, C. K.; Patrickios, C. S. Model Amphiphilic Polymer Conetworks in Water: Prediction of Their Ability for Oil Solubilization. *ACS Omega* **2019**, *4* (3), 4721–4738.
(23) He, C.; Erdodi, G.; Kennedy, J. P. Individual and Simultaneous Swelling of Amphiphilic Conetworks in Water Andn-Heptane. *J Polym Sci B Polym Phys* **2006**, *44* (10), 1474–1481.
(24) Yati, I.; Karadag, K.; Sonmez, H. B. Amphiphilic Poly(Ethylene Glycol) Gels and Their Swelling Features. *Polym Adv Technol* **2015**, *26* (6), 635–644.
(25) Kizil, S.; Bulbul Sonmez, H. Star PEG-Based Amphiphilic Polymers: Synthesis, Characterization and Swelling Behaviors. *Polymer Bulletin* **2019**, *76* (4), 2081–2096.
(26) Danforth, W. E. The Dielectric Constant of Liquids under High Pressure. *Physical Review* **1931**, *38* (6), 1224–1235.
(27) Leahy, D. E. Intrinsic Molecular Volume as a Measure of the Cavity Term in Linear Solvation Energy Relationships: Octanol-Water Partition Coefficients and Aqueous Solubilities. *J Pharm Sci* **1986**, *75* (7), 629–636.
(28) Vilas-Boas, S. M.; da Costa, M. C.; Coutinho, J. A. P.; Ferreira, O.; Pinho, S. P. Octanol–Water Partition Coefficients and Aqueous Solubility Data of Monoterpenoids: Experimental, Modeling, and Environmental Distribution. *Ind Eng Chem Res* **2022**, *61* (8), 3154–3167.
(29) Yalkowsky, S. H.; He, Y. Handbook of Aqueous Solubility Data: An Extensive Compilation of Aqueous Solubility Data for Organic Compounds Extracted from the AQUASOL DATAbASE; CRC Press, LLC: Boca Raton, FL, 2003; p 536.
(30) Haynes, W. M. CRC Handbook of Chemistry and Physics (97th Ed.); CRC Press, 2016; p 5164.
(31) Yalkowsky, S. H.; He, Y.; Jain, P. Handbook of Aqueous Solubility Data Second Edition; CRC Press: Boca Raton, FL, 2010; p 687.
(32) Yalkowsky, S. H.; He, Y. Handbook of Aqueous Solubility Data: An Extensive Compilation of Aqueous Solubility Data for Organic Compounds Extracted from the AQUASOL DATAbASE; CRC Press, LLC: Boca Raton, FL, 2003; p 326.
(33) Sander, U.; Wolf, B. A. Solubility of Poly(n-Alkylmethacrylate)s in Hydrocarbons and in Alcohols. *Die Angewandte Makromolekulare Chemie* **1986**, *139* (1), 149–156. https://doi.org/https://doi.org/10.1002/apmc.1986.051390114.

(34) Abe, M.; Yamazaki, T.; Ogino, K.; Kim, M. J. Phase Behavior and Physicochemical Properties of Sodium Octyl Sulfate/n-Decane/1-Hexanol/Aqueous Aluminum Chloride Middle-Phase Microemulsion. *Langmuir* **1992**, *8* (3), 833–837. https://doi.org/10.1021/la00039a017.
(35) Gradzielski, M.; Hoffmann, H.; Langevin, D. Solubilization of Decane into the Ternary System TDMAO/1-Hexanol/Water. *J Phys Chem* **1995**, *99* (33), 12612–12623. https://doi.org/10.1021/j100033a039.
(36) Sprouse, D.; Reineke, T. M. Investigating the Effects of Block versus Statistical Glycopolycations Containing Primary and Tertiary Amines for Plasmid DNA Delivery. *Biomacromolecules* **2014**, *15* (7), 2616–2628.
(37) Keiderling, U. The New "BerSANS-PC" Software for Reduction and Treatment of Small Angle Neutron Scattering Data. *Appl Phys A Mater Sci Process* **2002**, *74*, s1455–s1457.
(38) Vamvakaki, M.; Patrickios, C. S.; Lindner, P.; Gradzielski, M. Amphiphilic Networks Based on Cross-Linked Star Polymers: A Small-Angle Neutron Scattering Study. *Langmuir* **2007**, *23* (21), 10433–10437.
(39) Kegel, W. K.; Lekkerkerker, H. N. W. Phase Behaviour of an Ionic Microemulsion System as a Function of the Cosurfactant Chain Length. *Colloids Surf A Physicochem Eng Asp* **1993**, *76*, 241–248.
(40) Gradzielski, M. Effect of the Cosurfactant Structure on the Bending Elasticity in Nonionic Oil-in-Water Microemulsions. *Langmuir* **1998**, *14* (21), 6037–6044.
(41) Kortüm, G.; Vogel, W.; Andrussow, K. Dissociation Constants of Organic Acids in Aqueous Solution. *Pure and Applied Chemistry* **1960**, *1* (2–3), 187–536.